Submitted October 3, 2022;
accepted November 28, 2022.

Ernesto A. Lee, DMD
Hari Prasad, BS, MDT, MS
Samuel Lynch, DMD, DMSc

Sequential Human Histology Results of the Subperiosteal Minimally Invasive Aesthetic Ridge Augmentation Technique (SMART): A Chronologic Wound Healing Proof-of-Principle Study

Traditional GBR procedures have been associated with frequent complications and compromised peri-implant esthetics. Tunneling techniques have been proposed as a promising alternative in this regard. More recently, a subperiosteal minimally invasive aesthetic ridge augmentation technique (SMART) was reported to have been clinically successful in a prospective case series. This technique includes the use of a bone graft/recombinant human platelet-derived growth factor-BB combination delivered to the site by a tunneling method. However, published histologic information regarding the nature of the regenerated tissue has been limited. The current study evaluated the histologic and histomorphometric findings of four human specimens harvested at 2, 5, 9, and 14 months after ridge augmentation using the SMART method. Evaluations of the wound healing and bone regeneration sequence over time found that the ridge augmentation was the result of extensive new bone formation that progressed through the woven bone to lamellar bone stages, with remodeling of the xenogeneic graft material and replacement by patient bone. This is the first study utilizing sequential human specimens to histologically examine the chronology of wound healing following alveolar ridge augmentation. *Int J Periodontics Restorative Dent 2024;44:38–49. doi: 10.11607/prd.6559*

Guided bone regeneration (GBR) often results in incomplete wound closure and soft tissue dehiscences, leading to exposure of the membrane or graft material.[1] These complications negatively impact the peri-implant soft tissue morphology and the outcome of bone augmentation while increasing morbidity and treatment duration.

Esthetic outcomes in implant dentistry are dependent on the architecture of the peri-implant soft tissues.[2] Thus, the sequelae from GBR complications often lead to an unesthetic appearance.[3,4] These negative results are difficult to remedy, requiring restorative compromises that may be detrimental to implant maintenance and long-term peri-implant health.

Minimally invasive techniques offer the potential to decrease complications and morbidity while preserving the peri-implant soft tissue morphology. Early publications on tunneling bone grafting

by Block et al[5] and Block and Degen[6] focused on the augmentation of mandibular posterior edentulous ridges. Subsequently, Nevins et al treated edentulous spans of the anterior maxilla using recombinant human platelet-derived growth factor-BB (rhPDGF-BB) in combination with three different matrices delivered through a tunneling technique with promising results.[7]

More recently, a subperiosteal minimally invasive aesthetic ridge augmentation technique (SMART) reported clinical success in a prospective case series comprising 60 sites in 21 patients.[8] This technique includes the use of a tunneling method to deliver a bone graft/rhPDGF-BB combination to the site. The average gain in ridge width reported for all treatment categories was 5.11 ± 0.76 mm. Morbidity and complications were reduced as well.[8] However, there is limited information related to the histologic nature of the regenerated tissue using this technique, with only a single human biopsy sample available.

The purpose of this study was to histologically evaluate the chronology of bone regeneration in humans following alveolar ridge augmentation with SMART.

Materials and Methods

SMART procedures were performed on the patients by the first author (E.A.L.). Subjects were examined clinically, and treatment eligibility was determined through a review of their medical and dental history, intraoral condition, radiographs, and preoperative CBCT scans. Exclusion criteria were as follows: ASA physical status III or IV, substance abuse, uncontrolled diabetes, maxillary or mandibular radiation therapy, intravenous bisphosphonate therapy, pregnancy, untreated periodontal disease, presence of periapical cysts or abscesses, acute infections, and intraoral lesions.

Details of the surgical procedure and the risks and benefits were explained to the patients. Signed informed consent was obtained, including permission to harvest specimens for histologic analysis and publication and educational purposes. Subjects were prescribed 500 mg of amoxicillin three times per day for a 10-day period, with instructions to start taking the medication 2 days prior to surgery. Azithromycin or clindamycin was prescribed in cases of penicillin allergy. Calculus, biofilm, and food residue were removed preoperatively.

The SMART procedure was performed following the guidelines described in a previous publication.[8] Using a small remote incision, the soft tissue was elevated from the ridge to create a subperiosteal tunnel and pouch, which was then filled with a bone graft matrix mixed with a growth factor. In preimplant sites (Cases 2 to 4), anorganic bovine bone mineral (ABBM) was combined with a small fraction of freeze-dried mineralized bone allograft (FDBA) to promote graft integration. For the treatment of implant bone dehiscences (Case 1), ABBM was used without the addition of FDBA. All utilized biomaterials were hydrated with rhPDGF-BB (GEM 21S, Lynch Biologics) prior to grafting. No bone decortication procedures were performed. Space-maintaining devices and barrier membranes were not utilized.

The biopsy samples selected for this report were obtained 2, 5, 9, and 14 months after the SMART procedure. The four total patients comprised three women and one man, ranging from 32 to 84 years of age. Except for the 2-month specimen, all samples were collected at the time of implant placement. Specimens were chosen for this study based on two criteria. The first criterion was the selection of samples harvested at meaningful observation intervals to examine the chronologic progression of bone regeneration. The harvesting periods were not adjusted for investigational purposes but rather as a result of patient-related variables. The second selection criterion was based on the lack or minimal presence of native bone in an effort to obtain histomorphometry results representative of the percentage of bone in the grafted area. Consequently, the specimens selected were comprised entirely of grafted bone, except for the 5-month sample (Case 2), which included a small amount of native bone.

The biopsy samples were placed in 10% neutral buffered formalin and forwarded to the Hard Tissue Research Laboratory (University of Minnesota) where histologic processing and histomorphometric analysis were performed by the second author (H.P.).

Histologic Preparation

Upon receipt, the specimens were dehydrated with a graded series of alcohol for 9 days. Following dehydration, the specimens were infiltrated with a light-curing embedding resin (Technovit 7200 VLC, Kulzer). After 20 days of infiltration with constant shaking at normal atmospheric pressure, the specimens were embedded and polymerized by 450-nm light, and the temperature of the specimens never exceeded 40ºC. The specimens were then prepared using the Donath cutting/grinding method.[9,10] The specimens were cut to a thickness of 150 µm on an EXAKT Technologies cutting/grinding system. The specimen slides were then polished to a thickness of 45 to 65 µm using a series of polishing sandpaper discs (800 to 2,400 grit) using an EXAKT Technologies microgrinding system followed by a final polish with 0.3-µm alumina polishing paste. The slides were stained with Stevenel blue and Van Gieson picrofuchsin for histologic analysis by means of bright field and polarized microscopic evaluation. These compounds stain differentially as follows:

- Vital bone stains a bright red with variations in intensity depending on the bone maturity.
- Nonvital bone and osteoid stain bright green.
- Nuclei of cells (including osteoblasts, osteoclasts, and osteocytes) stain blue.
- Connective tissue stains various shades of green.

Histomorphometry

Following histologic preparation, the specimens were evaluated histomorphometrically. All specimens were digitized at the same magnification using an Eclipse 50i microscope (Nikon) and a SPOT INSIGHT 2 Mega Sample digital camera (Diagnostic Instruments). Histomorphometric measurements were completed using a combination of programs (Photoshop, Adobe; and ImageJ, National Institutes of Health). At least two slides of each specimen were evaluated. Histomorphometric analysis was performed, and the following parameters were measured in terms of the percentage of the total specimen area: vital bone, nonvital bone and new bone formation, residual graft material, and marrow space.

Results

Case 1: 2-Month Specimen

A 59-year-old woman was treated to regenerate bone over dehisced labial surfaces of implants at sites 45 and 47 (FDI numbering system). ABBM (Bio-Oss, Geistlich North America) mixed with rhPDGF-BB (GEM 21S) was placed over the implant surfaces and the adjacent unprepared cortical bone surface. Two months after the procedure, excess graft material was removed mesial to the implant at site 45 due to patient complaints of mental nerve paresthesia.

Sharp dissection was utilized to expose a firmly adherent mass with a spongy consistency containing ABBM particles. The mass was attached to the cortical bone surface, requiring the use of surgical chisels to harvest the specimen as a whole. Histologic analysis under polarized light revealed new bone formation advancing from the entire periphery of the graft, including the area facing the unprepared cortical bone (Fig 1).

Histomorphometry results yielded < 1% of bone and 42% residual xenograft (Table 1). This is consistent with the histologic appearance of the specimen and is to be expected at an early phase of the bone regeneration process.

A thin layer of new bone was observed on the surface of ABBM particles when seen at a high magnification (Fig 2). Bridging of the new bone was not observed at this early healing stage. The presence of newly formed bone on the entire specimen surface, including the area facing the unprepared cortical bone (see Fig 1c), is a significant observation that supports the hypothesis that, using this protocol, osteogenesis progressed from both the periosteum and the cortical bone surface.[11]

Case 2: 5-Month Specimen

An 84-year-old woman was treated for ridge augmentation at sites 36 and 37. Past history included extraction complications and implant failure. The utilized bone graft comprised ABBM (Bio-Oss) and FDBA hydrated with rhPDGF-BB (GEM 21S). A large volume of horizontally and vertically regenerated bone was achieved without complications via the SMART procedure. Five months later, a core measuring approximately

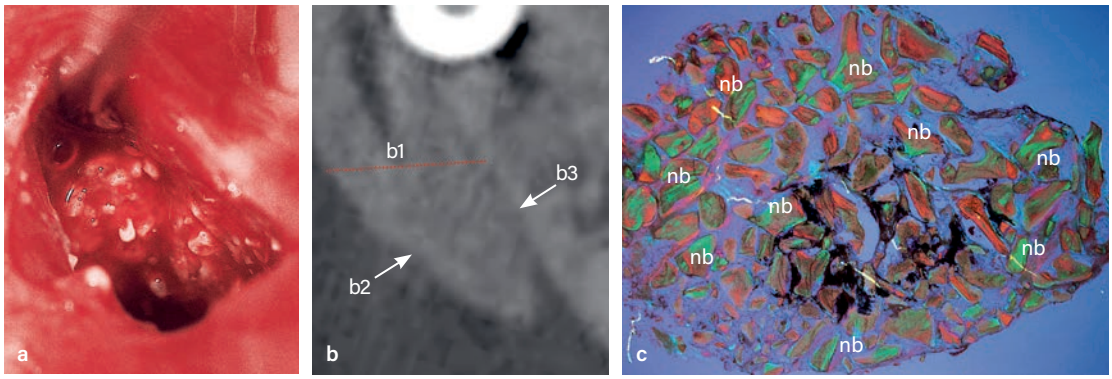

▲ **Fig 1** Case 1. *(a)* A mass of excess graft material containing ABBM granules was removed 2 months after augmentation. *(b)* The CT scan shows the location of the removed biomaterial, as well as bone resection (b1), the area of the graft facing the periosteum (b2), and the area of the graft facing the cortical bone surface (b3). *(c)* A higher magnification view (×20) using polarized microscopy reveals new bone (nb) on the entire periphery of the graft.

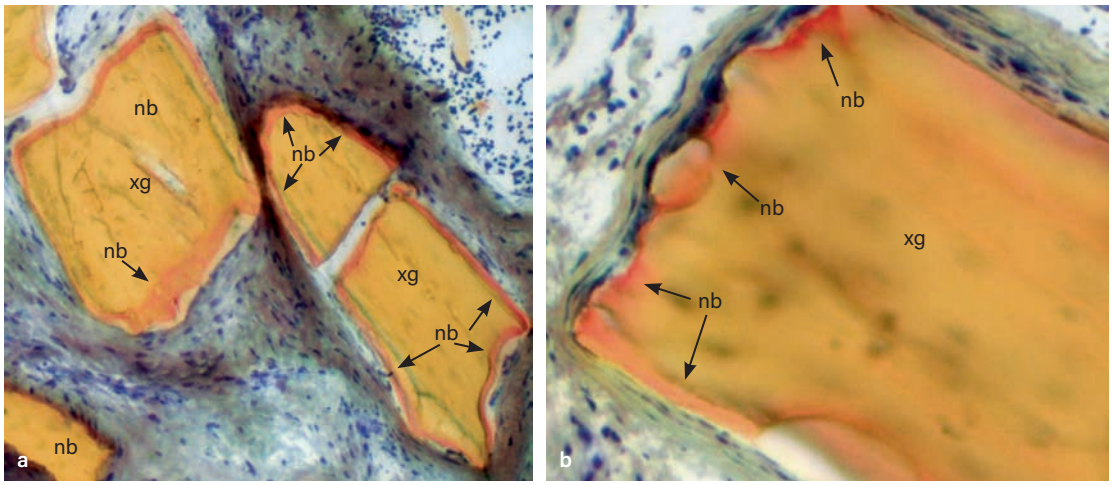

▲ **Fig 2** Case 1. *(a)* At ×100 magnification, a thin layer of newly formed bone (nb) can be observed surrounding ABBM particles (xg). Bridging of new bone has not taken place. *(b)* At ×200 magnification, new bone formation is evident.

4 × 5 mm was harvested using a trephine as part of the osteotomy preparation of site 37 (Figs 3a and 3b).

This is the only specimen in the study that included native bone. The transitional area between the graft and the native bone surface was evident (Figs 3a and 3c). Layers of new bone of varying thicknesses can be observed surrounding the ABBM and FDBA, coalescing into a network of regenerated

Table 1 Histomorphometric Results from the 2-Month Specimen

Variable	Megapixels, n	Percentage
Total specimen area	385,410	100%
Vital bone area	3,075	< 1%
FDBA area	0	0%
ABBM area	163,853	42%
Marrow/fibrous tissue area	218,482	57%

ABBM = anorganic bovine bone mineral; FDBA = freeze-dried bone allograft. The very low percentage of bone and high percentage of xenograft particles is expected at this early healing stage.

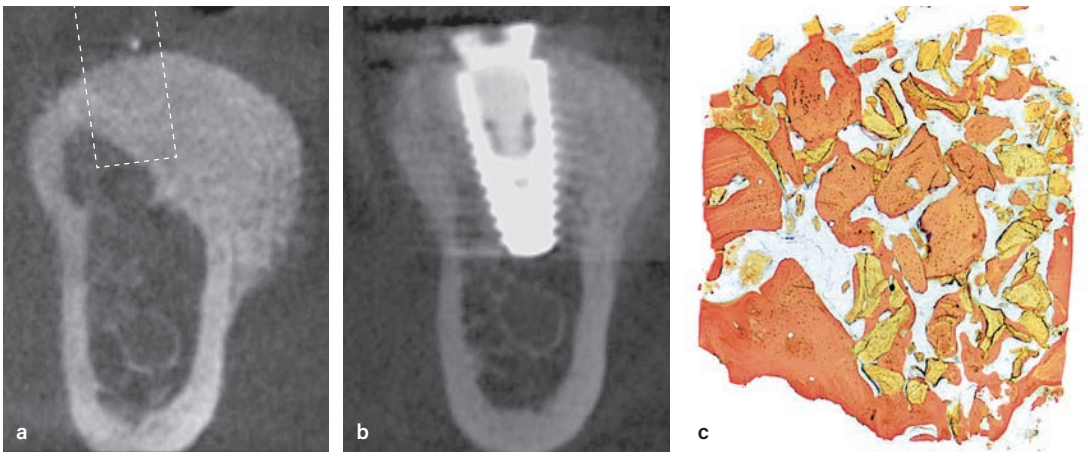

▲ **Fig 3** Case 2. *(a)* Appearance of an augmented ridge at site 18 and future site of the biopsy sample (*dotted line*). *(b)* A specimen was obtained during the osteotomy procedure, followed by implant placement. *(c)* Histologic appearance of the 4 × 5–mm core at ×20 magnification, viewed in the same orientation as it was harvested.

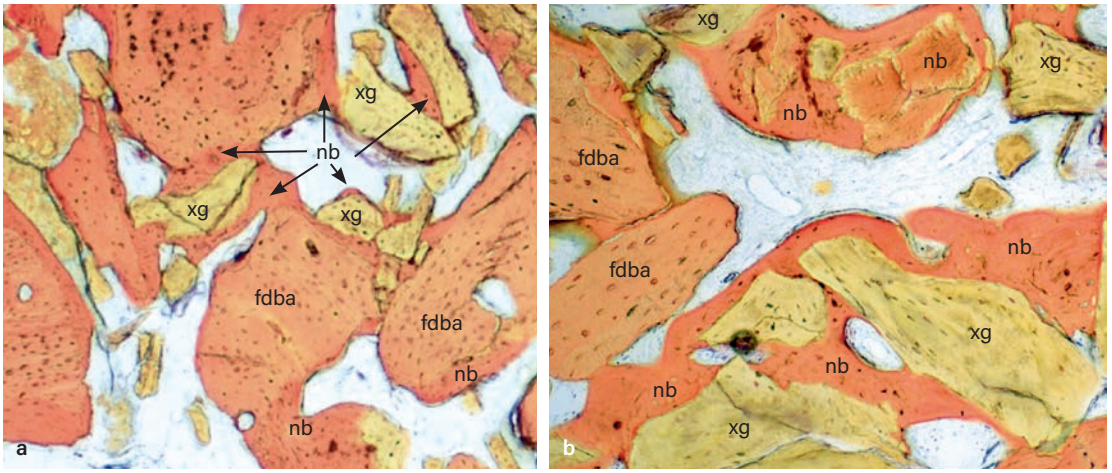

▲ **Fig 4** Case 2. Histologic views of the 5-month specimen at *(a)* ×40 and *(b)* ×100 magnifications show an extensive network of newly formed bone (nb) surrounding and bridging the mineralized allograft (fdba) and bovine xenograft particles (xg).

Table 2 Histomorphometric Results from the 5-Month Specimen

Variable	Megapixels, n	Percentage
Total specimen area	730,395	100%
Vital bone area	272,278	50%
FDBA area	95,437	26%
ABBM area	124,231	17%
Marrow/fibrous tissue area	238,449	33%

ABBM = anorganic bovine bone mineral; FDBA = freeze-dried bone allograft. The results suggest an accelerated turnover of ABBM at this stage and replacement with vital bone.

bone that bridged the biomaterial particles and was in direct apposition to the native bone surface (Fig 4).

The histomorphometric analysis revealed that while 50% of bone was present, only 17% of residual xenograft remained in the specimen. The relatively low amount of ABBM particles at this stage could be attributed to the accelerated turnover rate associated with rhPDGF-BB[12] (Table 2).

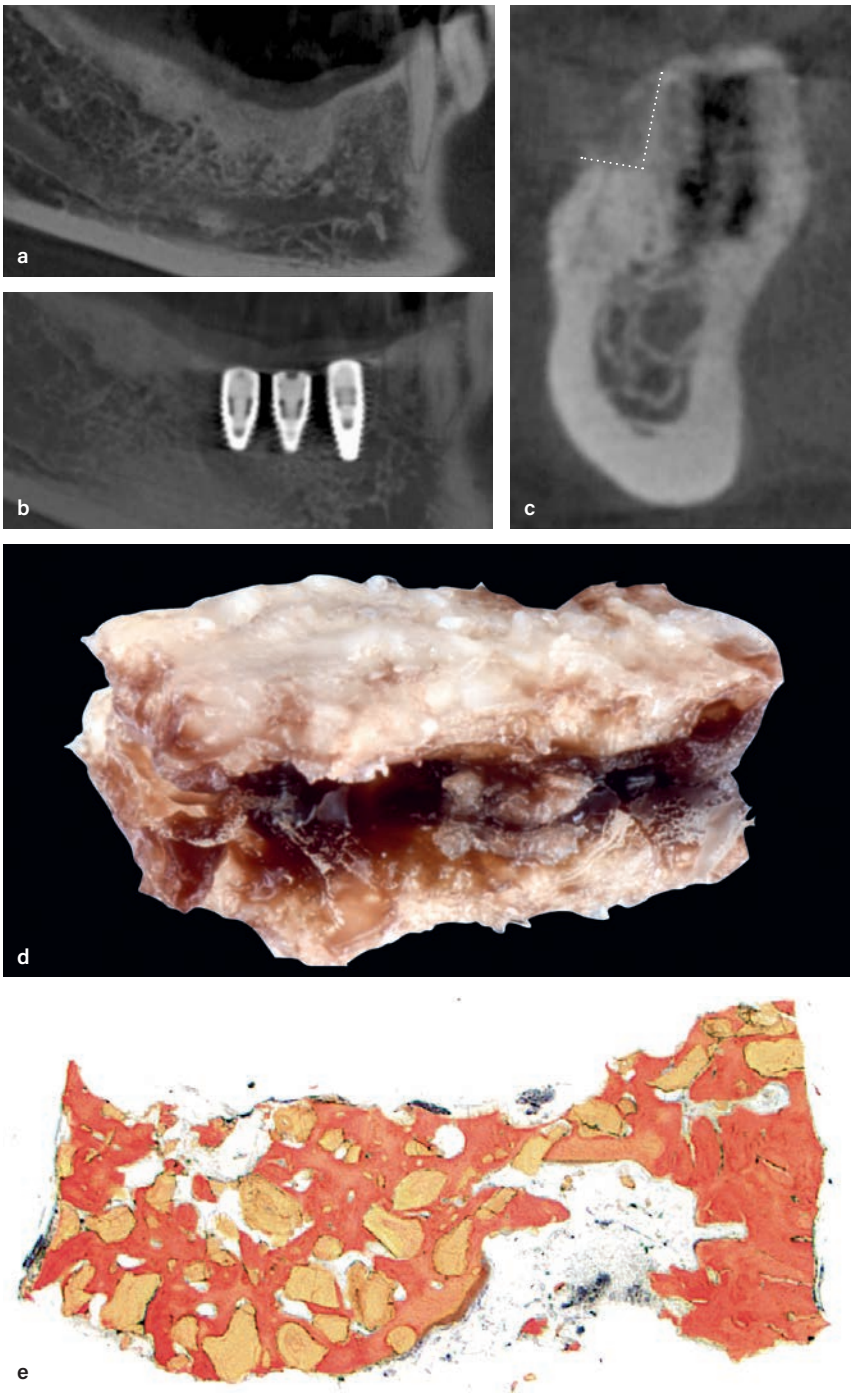

▶ **Fig 5** Case 3. *(a)* Preoperative radiographic appearance. *(b)* Results of ridge augmentation and implant placement 9 months later. *(c)* CT cross-sectional view of site 31, showing the donor area. *(d)* A wedge-shaped specimen was harvested from the grafted area. *(e)* Histologic appearance of the sample at ×20 magnification.

Case 3: 9-Month Specimen

A 67-year-old woman received ridge augmentation treatment in the mandibular right quadrant after the removal of previously failed implants. A combination of ABBM (Bio-Oss) and FDBA hydrated with rhPDGF-BB (GEM 21S) was utilized. Nine months after the procedure, a wedge-shaped specimen was harvested from site 47 during implant placement at sites 44, 45, and 46. The specimen was obtained from a grafted area and did not include any native bone (Fig 5).

Histologic evaluation revealed the presence of a well-established network of newly formed bone in direct apposition to the ABBM particles. The

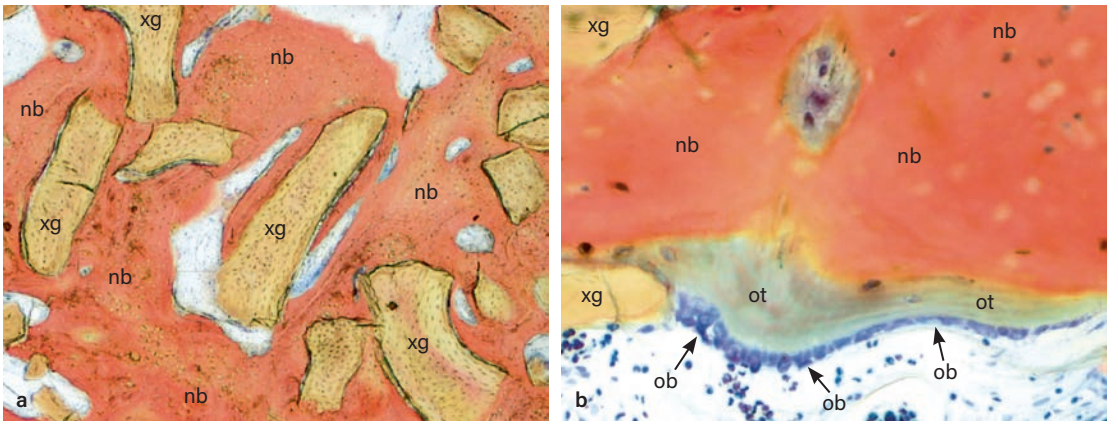

▲ **Fig 6** Case 3. *(a)* Histologic view of a section from the 9-month biopsy sample, viewed at ×40 magnification. Xenograft particles (xg) are encircled and linked by a broad network of newly formed bone (nb). The allograft has been resorbed and replaced with vital bone, while xenograft particles are undergoing progressive resorption. *(b)* At ×200 magnification, osteoblasts (ob) can be seen depositing a layer of osteoid tissue (ot) over the newly formed bone.

Table 3 Histomorphometric Results from the 9-Month Specimen

Variable	Megapixels, n	Percentage
Total specimen area	301,776	100%
Vital bone area	175,847	58%
FDBA area	0	0%
ABBM area	77,913	26%
Marrow/fibrous tissue area	48,736	16%

ABBM = anorganic bovine bone mineral; FDBA = freeze-dried bone allograft. A high percentage of new vital bone and a low percentage of residual ABBM particles were seen. FDBA particles were completely resorbed.

allograft particles were completely resorbed and replaced by vital bone. The thickening woven bone matrix encircled and linked the ABBM particles, concomitant with the progression of osteogenesis (Fig 6a). At ×200 magnification, osteoblasts can be observed depositing a layer of osteoid tissue on the surface of the newly formed bone (Fig 6b).

The histomorphometry results presented in Table 3 demonstrate 58% vital bone, which should be conducive to excellent implant stability. The absence of FDBA is evident at 9 months, while 26% of ABBM particles remain. The broader matrix of newly formed bone is the result of the complete resorption of the FDBA, continued remodeling of the ABBM, and replacement with vital bone.

Case 4: 14-Month Specimen

A 32-year old man presented for augmentation of a severely resorbed maxillary anterior ridge. The previous history included severe trauma at age 12, resulting in alveolar fractures and loss of teeth 22 through 24. Five implants placed at age 18 failed over time and required removal. A bone graft comprised of ABBM (SigmaGraft), and FDBA was hydrated with rhPDGF-BB (GEM 21S) and used to augment the severely deficient ridge. A large volume vertical and horizontal ridge augmentation was achieved without complications using the SMART procedure (Figs 7, 8a, and 8b).

Five implants were placed 14 months after bone augmentation (Fig 8c). During preparation of the osteotomies, a trephine bur was used to harvest a specimen (approximately 2.5 × 6 mm) from site 21 that was then sent for histologic analysis (Fig 9).

The dark staining exhibited by the ABBM particles in this specimen is useful as a histologic marker (see Fig 9c). The larger particles present in the apical portion of the core confirm that the sample is comprised entirely of vertically augmented bone. Residual ABBM particles of varying dimensions can be

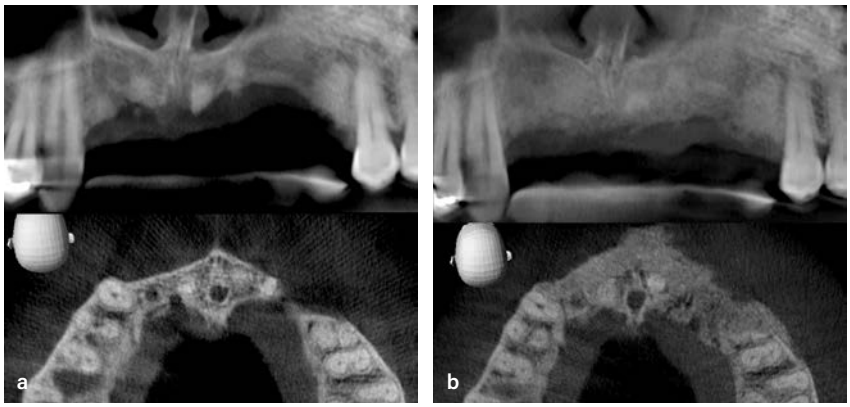

▶ **Fig 7** Case 4. *(a)* Severely resorbed maxillary anterior ridge due to trauma and the subsequent loss of 5 implants. *(b)* A large volume vertical and horizontal augmentation was achieved using the SMART procedure.

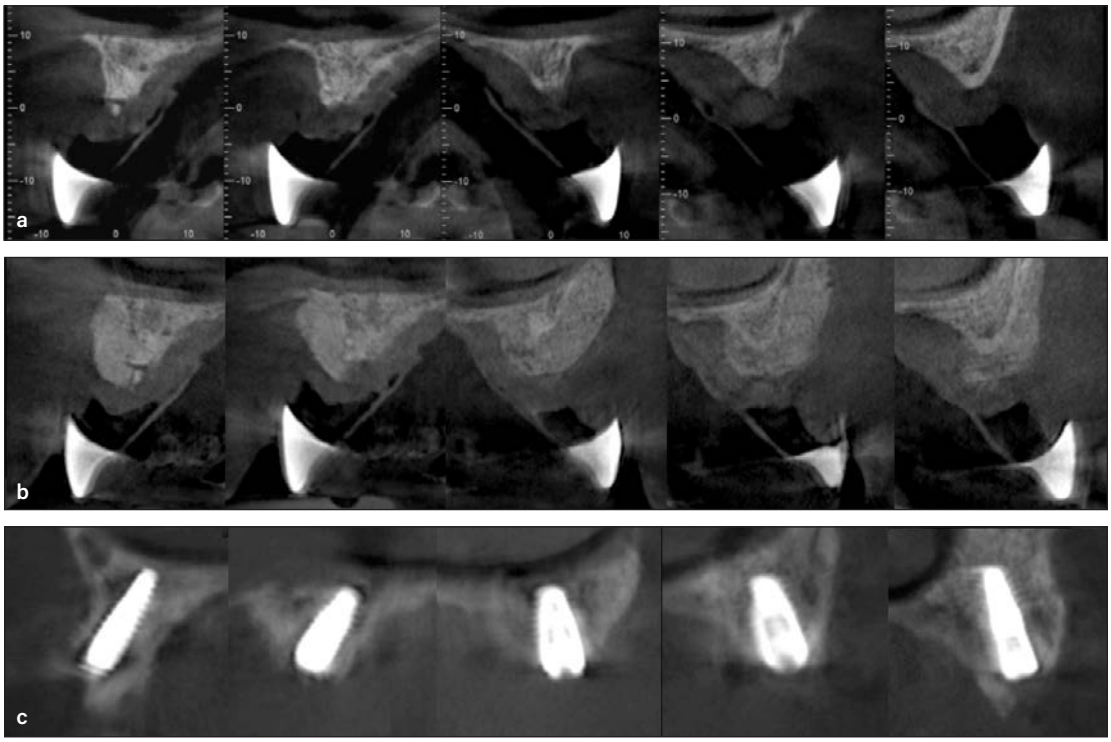

▲ **Fig 8** Case 4. *(a)* CBCT cross-sectional view of the pretreatment appearance of the deficient ridge. *(b)* At the 3-month postsurgical follow-up, substantial increases in vertical and horizontal dimensions can be seen. *(c)* Implants were placed at 14 months following the SMART procedure.

observed throughout the specimen. The abundance of minute dark particles is evidence that substantial turnover of the ABBM has taken place. Moving from the coronal to apical aspects, the particles decrease in size, indicating that biomaterial remodeling and integration progressed from the periphery of the graft (see Fig 9c).

High-magnification photomicrographs show residual xenograft particles completely embedded within a broad and dense matrix of newly formed bone (Fig 10a). The newly formed bone can be observed in direct apposition to the surfaces of the ABBM particles (Fig 10b). The histologic appearance under polarized light is one of vital, well-organized, functional bone (Fig 10c). The interstitial (il) and concentric lamellae (cl) observed are evidence that the regenerated bone underwent normal remodeling and maturation into cortical bone. The high mechanical resistance encountered during the osteotomy procedure suggests

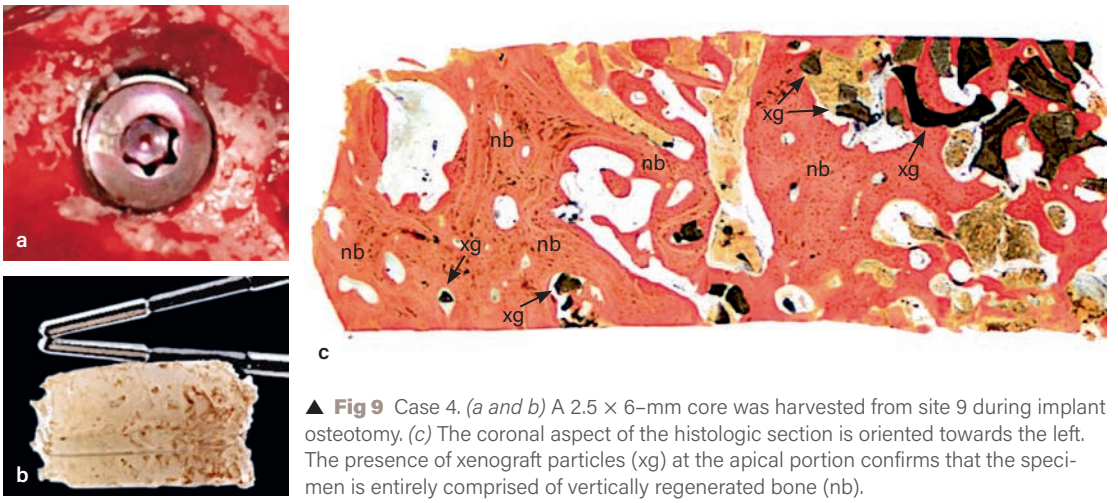

▲ **Fig 9** Case 4. *(a and b)* A 2.5 × 6–mm core was harvested from site 9 during implant osteotomy. *(c)* The coronal aspect of the histologic section is oriented towards the left. The presence of xenograft particles (xg) at the apical portion confirms that the specimen is entirely comprised of vertically regenerated bone (nb).

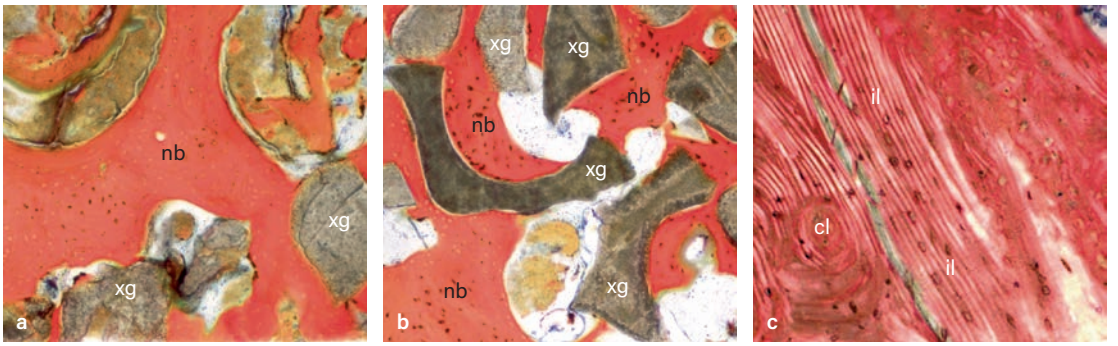

▲ **Fig 10** Case 4. *(a and b)* Photomicrographs at ×100 magnification reveal an abundance of newly regenerated bone (nb) in direct apposition to xenograft particles (xg) embedded within. *(c)* Interstitial (il) and concentric lamellae (cl) are visible under polarized light at ×100 magnification. This is consistent with the appearance of vital, well-organized, functional cortical bone.

Table 4 Histomorphometric Results from the 14-Month Specimen

Variable	Megapixels, n	Percentage
Total specimen area	653,053	100%
Vital bone area	396,640	61%
FDBA area	0	0%
ABBM area	51,347	8%
Marrow/fibrous tissue area	205,066	31%

ABBM = anorganic bovine bone mineral; FDBA = freeze-dried bone allograft. The amount of bone is higher than usual in the maxillary anterior region. The absence of FDBA and low percentage of residual ABBM are likely due to the effects of rhPDGF, which has been reported to accelerate resorption of bone graft particles and replacement with vital bone.

the presence of a thick layer of cortical bone.

Histomorphometric analysis found the sizable presence (61%) of regenerated vital bone (Table 4). This percentage is higher than that reported for the mineralized bone content in the maxillary anterior area[13] and is consistent with the substantial amount of newly formed bone visible in the histologic section. Additionally, FDBA particles were absent, and only 8% of residual xenograft remained. The small amount of ABBM particles is

most likely a result of the influence of the rhPDGF-BB over time, which has been reported to accelerate resorption of ABBM and new bone formation.[12]

Discussion

The sequential human histology presented herein provides chronologic information regarding the growth factor–mediated bone regeneration associated with the SMART procedure and challenges commonly held beliefs.

Traditional GBR principles are based on the use of barrier membranes to prevent epithelial proliferation into the biomaterial.[14] However, previous studies have demonstrated that membranes are not required in rhPDGF-BB–mediated regeneration and may actually be detrimental to new bone formation.[12,15] The periosteum has been documented as a source of stem cells, and the osteogenic potential of periosteum-derived cells has also been reported.[16,17] Interestingly, however, the 2-month specimen in this study exhibited newly formed bone around its entire periphery, including areas facing both the periosteum and the cortical bone. This was unexpected, as no decortication of the native bone was performed, indicating that osteoprogenitor cells were supplemented by sources other than the periosteum. Therefore, the existence of an rhPDGF-BB–mediated bone regeneration pathway is proposed, whereby perivascular stem cell precursors known as *pericytes* were responsible for new bone formation in the area of the graft opposing the unprepared cortical bone surface.[18]

In an early study, Díaz-Flores et al suggested that pericytes contribute a supplementary population of osteoprogenitor cells in new bone formation.[11] Scanning electron microscopy has since revealed the presence of pericytes on the abluminal surfaces of every blood vessel examined.[19] Additionally, the osteogenic potential of pericytes has been documented in vitro and in vivo.[20] Endogenous pericytes have been shown to differentiate into osteoblasts and osteocytes, contributing osteogenic cells to the healing of fractured bone.[21] When vascular injury occurs, pericytes are released from the blood vessels and are included in the extravasation, subsequently differentiating into stem cells (MSCs). PDGF signals and accelerates MSC migration to the injury site through its chemotactic properties, a phenomenon known as *cell homing*.[22] PDGF subsequently contributes to osteoblastic differentiation while also helping to stabilize the newly formed capillaries that drive the cascade of new bone formation. It is thus reasonable to suggest that the presence of rhPDGF-BB in the bone graft provided the signaling and stimuli necessary for osteogenesis to occur in the area of the graft facing the unprepared cortical bone surface.[23]

Simion et al reported a lack of new bone in the central portion of ABBM blocks treated with rhPDGF-BB during ridge augmentation procedures in dogs and suggested the incomplete saturation of the ABBM block with the PDGF as a possible factor.[12] Observations of the 2-month specimen in the present study revealed that new bone formation was initiated from the periphery of the graft. The 5-month and 9-month samples exhibited new bone present throughout both specimens. Additionally, the resorption pattern of the ABBM particles in the 14-month sample clearly demonstrates that remodeling progressed from the periphery to the central portion of the graft. This is supported by Lindhe et al, who reported the presence of woven bone in the central portion of healed extraction sockets,[13] and Schenk, who observed that healing of the middle portion always lagged behind the periphery of the wound in bone repair.[24] The present findings therefore suggest that the lack of newly formed bone in the central portion of the graft, reported by Simion et al[12] may be a function of the time of observation rather than the effect of incomplete saturation of the biomaterial with rhPDGF-BB.

Although the sample size of the present study is small, the histomorphometry results clearly demonstrate certain trends in the wound-healing progression from the 2-month to the 14-month specimen. A positive correlation was identified between the percentage of bone and healing time. Conversely, the percentage of ABBM decreased over time (Table 5). These findings are consistent with the histologic images that

Table 5 Sequential Chronologic Comparison of All Histomorphometric Results from the 14-Month Specimen

	2 mo (Sites 21 + 34) ABBM+PDGF	5 mo (Sites 19 + 36) ABBM+FDBA+PDGF	9 mo (Sites 31 + 47) ABBM+FDBA+PDGF	14 mo (Sites 9 + 21) ABBM+FDBA+PDGF
Megapixels, n				
Total specimen area	385,410	730,395	301,776	653,053
Vital bone area	3,075	272,278	175,847	396,640
FDBA area	0	95,437	0	0
ABBM area	163,853	124,231	77,913	51,347
Marrow/fibrous tissue area	218,482	238,449	48,736	205,066
Percentage				
Bone	< 1%	50%	58%	61%
FDBA	0%	26%	0%	0%
ABBM	42%	17%	26%	8%
Marrow/fibrous tissue	57%	33%	16%	31%

ABBM = anorganic bovine bone mineral; FDBA = freeze-dried bone allograft; PDGF = platelet-derived growth factor. The bone percentage increased over time, while the percentage of ABBM decreased as the healing period increased.

show increasing amounts of newly formed bone as time progresses, with decreasing amounts of ABBM and smaller particle sizes in more mature specimens.

Considering the percentages of bone reported in the present histomorphometry, it is important to note that all but one specimen was comprised solely of grafted bone. The 5-month specimen in Case 2 included a small amount of native bone (see Fig 3).

Conclusions

This study provides a histologic proof of principle that vertical and horizontal ridge augmentation can be achieved using the SMART procedure. The data presented documents the chronologic changes in percentages of vital bone, FDBA, and ABBM, as well as the formation of new bone resulting from this grafting technique. The results demonstrate that ABBM resorbs at a faster rate when used in combination with rhPDGF-BB and is subsequently replaced by regenerated bone. The cases reported herein illustrate the potential for creating large volumes of bone for the treatment of challenging 3D defects, without complications, using this minimally invasive technique. This is the first study that utilizes sequential human specimens to histologically examine the chronology of bone regeneration following alveolar ridge augmentation.

Acknowledgments

Dr Ernesto Lee is the Founder and CEO of SMART Biomedical. Dr Samuel Lynch is the Founder, CEO, and Chairman of Lynch Biologics. Dr Hari Prasad reports no conflicts of interest.

References

1. Jensen AT, Jensen SS, Worsaae N. Complications related to bone augmentation procedures of localized defects in the alveolar ridge. A retrospective clinical study. Oral Maxillofac Surg 2016;20:115–122.
2. Furhauser R, Florescu D, Benesch T, Haas R, Mailath G, Watzek G. Evaluation of soft tissue around single-tooth implant crowns: The pink esthetic score. Clin Oral Implants Res 2005;16:639–644.

3. Cosyn J, Eghbali A, Hanselaer L, et al. Four modalities of single implant treatment in the anterior maxilla: A clinical, radiographic and aesthetic evaluation. Clin Implant Dent Relat Res 2013;15:517–530.
4. Cosyn J, Sabzevar MM, De Bruyn H. Predictors of inter-proximal and midfacial recession following single implant treatment in the anterior maxilla: A multivariate analysis. J Clin Periodontol 2012;39:895–903.
5. Block MS, Kent JN, Ardoin RC, Davenport W. Mandibular augmentation in dogs with hydroxylapatite combined with demineralized bone. J Oral Maxillofac Surg 1987;45:414–420.
6. Block MS, Degen M. Horizontal ridge augmentation using human mineralized particulate bone: Preliminary results. J Oral Maxillofac Surg 2004;62(9 suppl 2):67–72.
7. Nevins ML, Camelo M, Nevins M, et al. Minimally invasive alveolar ridge augmentation procedure (tunneling technique) using rhPDGF-BB in combination with three matrices: A case series. Int J Periodontics Restorative Dent 2009;29: 371–383.
8. Lee EA. Subperiosteal minimally invasive ridge augmentation technique (S.M.A.R.T.): A new standard for bone reconstruction of the jaws. Int J Periodontics Restorative Dent 2017;37:165–173.
9. Rohrer MD, Schubert CC. The cutting-grinding technique for histological preparation of undecalcified bone and bone-anchored implants: Improvement in instrumentation and procedures. Oral Surg Oral Med Oral Pathol 1992;74:73–78.
10. Donath K, Breuner G. A method for the study of undecalcified bones and teeth with the attached soft tissues: The Sage Schliff (sawing and grinding) technique. J Oral Pathol 1982;11:318–326.
11. Diaz-Flores L, Gutierrez R, Lopez-Alonso A, Gonzalez R, Varela H. Pericytes as a supplementary source of osteoblasts in periosteal osteogenesis. Clin Orthop Relat Res 1992;(275)280–286.
12. Simion M, Rocchietta I, Kim D, Nevins M, Fiorellini J. Vertical ridge augmentation by means of deproteinized bovine bone block and recombinant human platelet-derived growth factor-BB: A histologic study in a dog model. Int J Periodontics Restorative Dent 2006;26:415–423.
13. Lindhe J, Bressan E, Cecchinato D, Corrá E, Toia M, Liljenberg B. Bone tissue in different parts of the edentulous maxilla and mandible. Clin Oral Implant Res 2013;24:372–377.
14. Dahlin C, Gottlow J, Lindhe A, Nyman S. Healing of maxillary and mandibular bone defects using a membrane technique. An experimental study in monkeys. Scand J Plast Reconstr Surg Hand Surg 1990;24:13–19.
15. Nevins M, Camelo M, Nevins ML, Schenk RK, Lynch SE. Periodontal regeneration in humans using recombinant human platelet-derived growth factor-BB (rhPDGF-BB) and allogeneic bone. J Periodontol 2003;74:1282–1292.
16. Zhu SJ, Choi BH, Huh JY, Jung JH, Kim BY, Lee SH. A comparative qualitative histological analysis of tissue-engineered bone using bone marrow mesenchymal stem cells, alveolar bone cells, and periosteal cells. Oral Surg Oral Med Oral Pathol Oral Radiol Endod 2006;101:164–169.
17. Ceccarelli G, Graziano A, Benedetti L, et al. Osteogenic potential of human oral-periosteal cells (PCs) isolated from different oral origin: An in vitro study. J Cell Physiol 2016;231:607–612.
18. Lynch SE. The role of growth factors in periodontal repair and regeneration. In: Polson AM (ed). Periodontal Regeneration: Current Status and Directions. Quintessence, 1994:179–198.
19. Caplan AI. New MSC: MSCs as pericytes are sentinels and gatekeepers. J Orthop Res 2017;35:1151–1159.
20. Doherty MJ, Ashton BA, Walsh S, Beresford JN, Grant ME, Canfield AE. Vascular pericytes express osteogenic potential in vitro and in vivo. J Bone Miner Res 1998;13:828–838.
21. Supakul S, Yao K, Ochi H, et al. Pericytes as a source of osteogenic cells in bone fracture healing. Int J Mol Sci 2019;20:1079.
22. Lynch SE, Marx RE, Nevins M, Wisner-Lynch LA. Tissue Engineering: Applications in Oral and Maxillofacial Surgery and Periodontics. Chicago: Quintessence, 2008.
23. Caplan AI, Correa D. PDGF in bone formation and regeneration: New insights into a novel mechanism involving MSCs. J Orthop Res 2011;29:1795–1803.
24. Schenk RK. Bone regeneration: Biologic basis. In: Buser D, Dahlin C, Schenk RK (eds). Guided Bone Regeneration in Implant Dentistry. Chicago: Quintessence, 1994:49–100.

Ernesto A. Lee, DMD
SMART Biomedical, Private Practice, Bryn Mawr, Pennsylvania, USA.

Hari Prasad, BS, MDT, MS
Hard Tissue Research Laboratory, University of Minnesota School of Dentistry, Minneapolis, Minnesota, USA.

Samuel Lynch, DMD, DMSc
Lynch Biologics, Franklin, Tennessee, USA.

Correspondence to:
Dr Ernesto A. Lee, drernestolee@gmail.com